

Many-Body Effects in Angle-Resolved Photoemission: Quasiparticle Energy and Lifetime of a Mo(110) Surface State

T. Valla,¹ A. V. Fedorov,¹ P. D. Johnson,¹ and S. L. Hulbert²

¹*Department of Physics, Brookhaven National Laboratory, Upton, New York 11973-5000*

²*National Synchrotron Light Source, Brookhaven National Laboratory, Upton, New York 11973-5000*

(Received 28 January 1999)

In a high-resolution photoemission study of a Mo(110) surface state various contributions to the measured width and energy of the quasiparticle peak are investigated. Electron-phonon coupling, electron-electron interactions, and scattering from defects are all identified mechanisms responsible for the finite lifetime of a valence photohole. The electron-phonon induced mass enhancement and rapid change of the photohole lifetime near the Fermi level are observed for the first time.

PACS numbers: 79.60.Bm, 73.20.At

Recent investigations of strongly correlated electron systems have questioned the validity of one of the most fundamental paradigms in solid state physics—Fermi liquid theory. The latter picture is based on the existence of “quasiparticles,” or single-particle-like low energy excitations which obey the exclusion principle and have lifetimes long enough to be considered as particles. Strictly speaking, the quasiparticle concept is restricted to zero temperature and a narrow region around the Fermi level [1], but its usefulness often continues to finite temperatures, and energies away from the Fermi level [2]. Indications for possible non-Fermi-liquid behavior have been found in some organic one-dimensional conductors [3] and in the normal state of high temperature superconductors [4]. A whole variety of experimental techniques have been employed in the search for such behavior, including resistivity measurements [5], infrared spectroscopy [6], scanning tunneling spectroscopy [7], and time-resolved two-photon photoemission [8]. Angle-resolved photoemission spectroscopy (ARPES) has an advantage, in that the energy and lifetime of the photohole are directly observable in the experiment. ARPES in principle measures the quasiparticle spectral function [9]:

$$A(\mathbf{k}, \omega) \propto \frac{\text{Im}\Sigma(\mathbf{k}, \omega)}{[\omega - \varepsilon_{\mathbf{k}} - \text{Re}\Sigma(\mathbf{k}, \omega)]^2 + [\text{Im}\Sigma(\mathbf{k}, \omega)]^2}, \quad (1)$$

where $\varepsilon_{\mathbf{k}}$ represents the energy of the state in the Hartree potential, and $\Sigma(\mathbf{k}, \omega)$ is the quasiparticle self-energy reflecting many-body interactions. Thus, momentum resolved self-energies are directly accessible in the experiment and, as such, ARPES represents a crucial experimental probe for the presence or absence of Fermi liquid behavior. Furthermore, complications connected to the lifetime of the photoelectron (in three-dimensional systems) may be overcome in quasi-low-dimensional systems. Indeed, there have already been several photoemission studies which quantitatively compare peak widths to calculated lifetimes for metallic surface states [10] and two-dimensional states in layered materials [11].

When considering the lifetime of the valence hole, there are three main decay mechanisms: electron-electron scattering, electron-phonon scattering, and impurity (defect) scattering. In three-dimensional systems, the *electron-electron* interaction contributes to the total width or inverse lifetime with the term $\Gamma_{e-e}(\omega, T) = 2\beta[(\pi k_B T)^2 + \omega^2]$. This scattering rate does not depend on the form of the interaction, but it may depend on the shape of the Fermi surface. If the scattering process is two dimensional, then the quadratic energy (temperature) dependence is modified by a logarithmic factor [12]. Previous attempts to observe this term for “prototypical” Fermi liquids, free-electron-like metals, have failed because β is often too small. Indeed, with estimated values of $\sim 10^{-2} \text{ eV}^{-1}$ for β , Γ_{e-e} contributes less than 5 meV variation through the whole band for the surface states studied [10]. Further, the temperature dependent contribution is negligible, being of the order of 0.1 meV at room temperature. The *electron-phonon* scattering contribution to the inverse lifetime, $\Gamma_{e-ph}(\omega, T)$ is given by

$$2\pi \int_0^\infty d\nu \alpha^2 F(\nu) [2n(\nu) + f(\nu + \omega) + f(\nu - \omega)], \quad (2)$$

where $\alpha^2 F(\omega)$ is the Eliashberg coupling function, and $f(\omega)$ and $n(\omega)$ are the Fermi and Bose-Einstein functions. This term monotonically increases with energy over the region $|\omega| < \omega_{\text{max}}$ (for $T = 0$), where ω_{max} is the cut-off of the phonon spectrum. The exact functional form is slightly dependent on the phonon spectrum. The temperature dependence of Γ_{e-ph} is approximately linear at higher temperatures, with slope $2\pi\lambda k_B$, where λ is the electron-phonon coupling constant. For most metals, $20 \text{ meV} < \omega_{\text{max}} = \omega_D < 100 \text{ meV}$ and λ falls between 0.1 and 1.5. *Impurity* scattering is elastic if the energy gap between the impurity ground state and its lowest excited state is large compared with the hole energy. To a first approximation, it is proportional to the impurity concentration, but independent of energy or temperature. Thus, at sufficiently low temperature in any real system, it will be the dominant decay mechanism for the hole close to E_F .

If the scattering mechanisms are independent, the total scattering rate is given by $\Gamma_{\text{tot}} = \Gamma_{e-e} + \Gamma_{e-ph} + \Gamma_{e-i}$. Virtually all temperature dependence in Γ_{tot} reflects the Γ_{e-ph} term, while any energy dependence falls within two distinct regions. In a narrow region $|\omega| \leq \omega_D$ (at $T = 0$) the only significantly varying term is Γ_{e-ph} . Any measurable change out of that region is most likely due to the Γ_{e-e} term. The real part of the quasiparticle self-energy is also known for all three mechanisms of scattering. Of these, electron-phonon coupling is the only term which is able to alter the quasiparticle mass in a narrow energy region around the Fermi level.

In the present paper, we report a detailed study of the lifetime effects associated with photoexcitation of a surface state on the Mo(110) surface. The electronic structure of this surface has already been the subject of several studies [13]. Our own tight-binding calculations in the slab formulation reproduce the presence of d -derived surface states or resonances in the midregion of the $\bar{\Gamma}$ - \bar{N} and $\bar{\Gamma}$ - \bar{H} lines, and indicate a bandwidth of 1–2 eV. It is well established that the line shape or width of a photoemission peak associated with excitation from such states reflects the lifetime of the photohole and is independent of any momentum broadening associated with the photoelectron [14]. However, the fact that bulk states are available for the surface state photohole to scatter into means that the three-dimensional decay rates are applicable even in the present case.

The experiment was carried out at the National Synchrotron Light Source, using the vacuum ultraviolet undulator beam line U13UB, which is based on a 3-m normal incidence monochromator. The photon energy used in the study was 15.16 eV. The electron analyzer was a Scienta SES-200, which uses a two-dimensional microchannel plate as a detector. The detector collects simultaneously a wide energy window and a wide angular window ($\sim 12^\circ$) of excited photoelectrons. This greatly reduces the time needed for data acquisition. The spread of the UV light was less than 2 meV, and the energy resolution of the electron analyzer was around 5 meV. The combined energy resolution therefore makes a minimal contribution to widths observed in this study. The angular resolution is $\sim 0.1^\circ$ which contributes 10 to 15 meV to the width of the studied state. The sample was cleaned by oxidation cycles (at 1400 K in an oxygen atmosphere of $\sim 5 \times 10^{-6}$ Pa), followed by flashes to ~ 2200 K. The sample temperature was measured with a W-WRe thermocouple. The base pressure was 4×10^{-9} Pa, more than 90% of which was hydrogen.

Figure 1 shows a typical spectrum of the Mo(110) surface, taken along the $\bar{\Gamma}$ - \bar{N} symmetry line, with the sample held at 70 K. The state shown in the figure corresponds to the surface resonance which closes the elliptical hole Fermi orbit around $\bar{\Gamma}$ [13]. The spectrum in the inset that shows a narrow energy region close to the Fermi level was taken in a short time interval, 1 min. Such short measuring intervals are required because, as shown later,

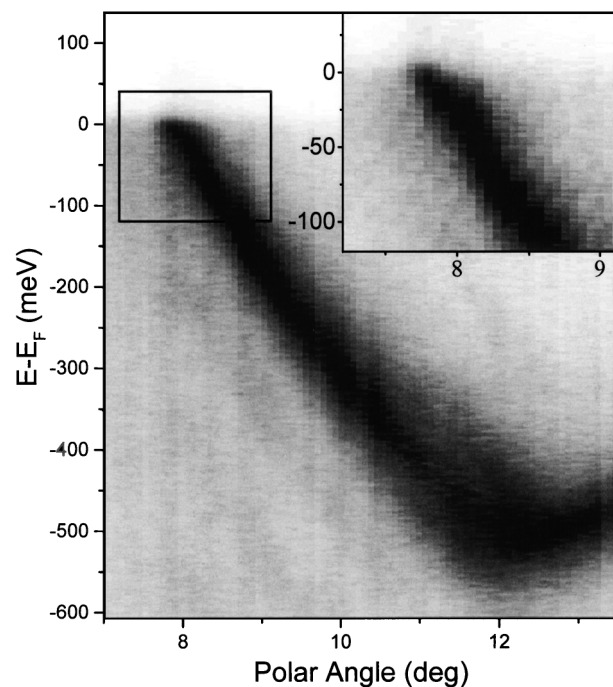


FIG. 1. ARPES intensity plot of the Mo(110) surface recorded along the $\bar{\Gamma}$ - \bar{N} line of the surface Brillouin zone at 70 K. Shown in the inset is the spectrum of the region around k_F taken with special attention to the surface cleanliness.

there is a significant influence from adsorption of residual gases. Important observations can be made directly from the spectrum shown in the inset: the state sharpens up on going towards the Fermi level, and there is an obvious change in band velocity near E_F . We focus our attention on these observations. Quantitative analysis is performed by taking slices through the spectrum, either at constant emission angle (vertical cut), or at constant energy (horizontal cut) to obtain the spectral intensity as a function of energy or emission angle, respectively. The two methods are equivalent in the sense that they provide information on the same $A(\mathbf{k}, \omega)$. However, analyzing the data by taking slices at constant energies is often more convenient because it is not affected by the Fermi distribution in the same way that slices at constant angle are. In our analysis we have used horizontal cuts to extract the dispersion, and vertical cuts to extract the width of the quasiparticle peak.

Figure 2 shows representative spectra obtained by slicing the spectral intensity in the vertical direction. Spectra are divided by an experimentally determined Fermi cutoff. The analysis was performed by fitting the spectra to Lorentzian peaks with a small linear background. The high-energy limit for the fitting interval was always below $\omega = 3k_B T$. Influences of the three experimental parameters (a) binding energy, (b) temperature, and (c) hydrogen exposure are shown, one being varied as the other two are kept constant. The trends are obvious: The width increases with all three parameters.

The energy dependence of the quasiparticle peak width is shown in Fig. 3. The error bars are statistical

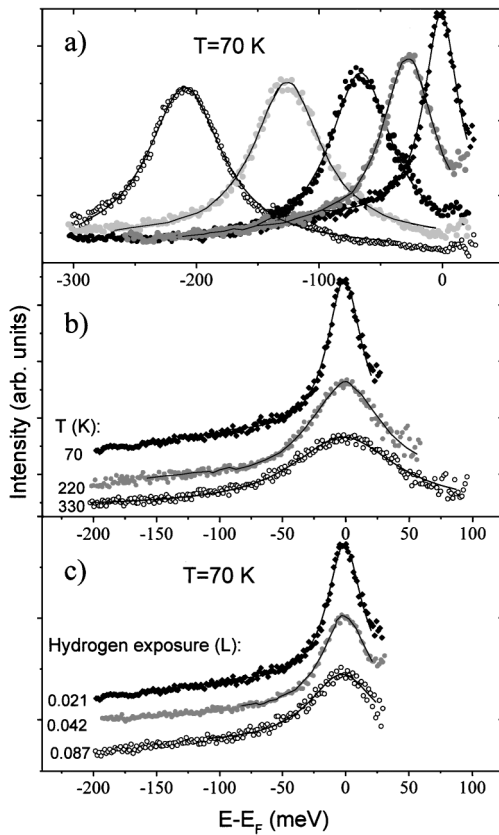


FIG. 2. Spectral intensity as a function of binding energy for constant emission angle, normalized to the experimentally determined Fermi cutoff. Data are symbols, while lines are fits to the Lorentzian peaks with a linear background. The dependence on the (a) binding energy, (b) temperature, and (c) hydrogen exposure is shown.

uncertainties from the fits. The peak width shows a minimum at $\omega = 0$, a sharp increase within the interval $0 > \omega > -40$ meV, followed by a slower increase at higher binding energies. The same behavior is also found for the angular peak width (horizontal cuts). At the same temperature, all spectra show the same dependence, offset by a constant value, dependent on the surface impurity level. The sharp increase in width near the Fermi level reflects the electron-phonon scattering. This is confirmed if we compare the experimental points with Γ_{e-ph} calculated from Eq. (2), using a theoretical $\alpha^2 F(\omega)$ for bulk molybdenum [15]. Both the range and magnitude of the increase agree well with calculation, suggesting that the theoretical bulk electron-phonon coupling constant from Ref. [15], $\lambda = 0.42$, applies also to the surface studied here. Further, the surface Debye energy is similar to the bulk value (≈ 30 meV), in accordance with recent measurements of surface phonon dispersions [16]. To obtain the agreement between the experimental points and the theoretical curve it was necessary to shift the latter uniformly by 26 meV. We attribute this difference to impurity scattering. The observation that the experimental points shift uniformly by the same amount is an indication that the impurity

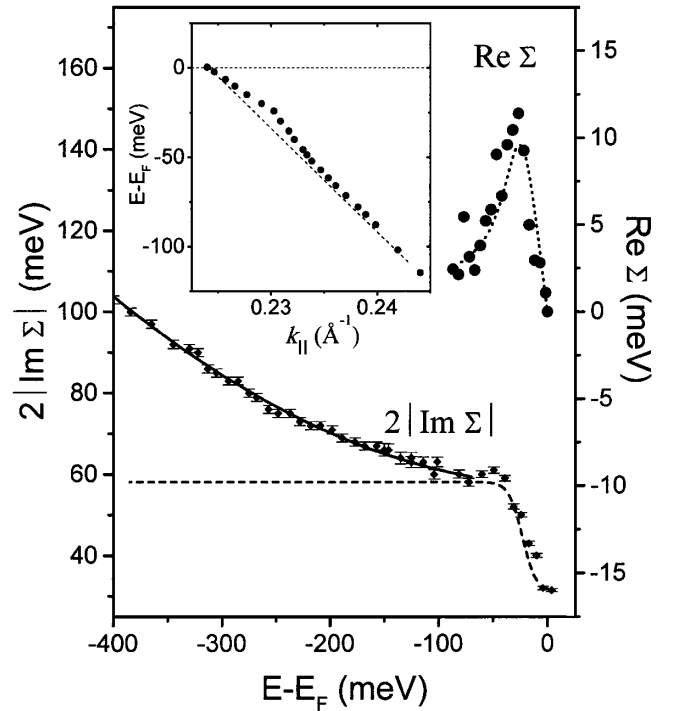


FIG. 3. The photohole self-energy as a function of binding energy at 70 K. The real part is obtained from the dispersion shown in the inset. The imaginary part is obtained from the width of the quasiparticle peak. The solid line is a quadratic fit to the high-binding energy data ($\omega < -80$ meV). The dashed (dotted) line shows the calculated electron-phonon contribution to the imaginary (real) part of the self-energy. The dashed line is shifted by 26 meV.

scattering is independent of energy. If we subtract the calculated electron-phonon contribution from the total width, we are left with a monotonic increase in binding energy that can be fitted with a parabola. This component is the electron-electron scattering term, with coefficient $2\beta \approx 0.28$ eV $^{-1}$. Within the Born approximation, $2\beta \approx (\pi U^2)/(2W^3)$. Our result is consistent with the on-site Coulomb repulsion $U \approx 0.6$ eV predicted for molybdenum [17] if we equate W with the bandwidth of the surface state (≈ 1.3 eV).

Also shown in Fig. 3 is the real part of the quasiparticle self-energy. Experimentally, it is obtained by subtracting a straight line from the measured dispersion of the quasiparticle peak (as shown in the inset of Fig. 3). In this energy range the straight line represents a good approximation for the dispersion of the “noninteracting” system (i.e., the system without electron-phonon coupling). It is chosen to have the same k_F as the quasiparticle dispersion and to match the quasiparticle dispersion in the range $\omega \approx -100$ meV. This procedure gives only the electron-phonon term for the real part of the self-energy. The component reflecting the electron-electron interaction stays hidden in the dispersion of the “noninteracting” system. Also shown is the electron-phonon contribution to the real part of the self-energy, obtained via the Kramers-Kronig transformation of the calculated imaginary part.

Figure 4 shows the width of the quasiparticle peak (a) as a function of temperature and (b) as a function of hydrogen exposure θ for two different binding energies. In Fig. 4(a), we also show electron-phonon contributions calculated from (2), and shifted up by 26 meV. The excellent agreement with the experimental points confirms that the temperature dependence reflects the electron-phonon interaction. Linear fits to the experimental data points produce different values for the electron-phonon coupling constant for the two binding energies: $\lambda = 0.52$ (at $\omega = 0$) and $\lambda = 0.35$ (at $\omega = 100$ meV), compared to the theoretical value of 0.42.

The observation that the width of the quasiparticle peak always has a significant constant term indicating the presence of impurity scattering leads to further investigation. It is known that this surface state is very sensitive to hydrogen adsorption. Figure 4(b) shows how the width of the state changes with the exposure to residual hydrogen (the exposure is determined as a product of background hydrogen pressure and time elapsed after flashing the sample to 2200 K). Note that the width saturates with exposure θ . If the scattering rate is proportional to the concentration of adsorbed particles, the experimental points become a measure of the concentration. Since the number of free adsorption sites decays exponentially with exposure, the concentration of adsorbed atoms as a function of exposure should change as $c(\theta) = c_0 + c_{\text{sat}}(1 - e^{-p\theta})$, where p is the adsorption probability and c_0 (c_{sat}) is the initial (saturation) concentration. The width of the quasiparticle peak can be fitted with the same dependence (solid lines). It is notable that extrapolation to zero exposure results in a residual width of 6 ± 5 meV at $\omega = 0$. Electron-phonon coupling contributes with ≈ 5 meV for

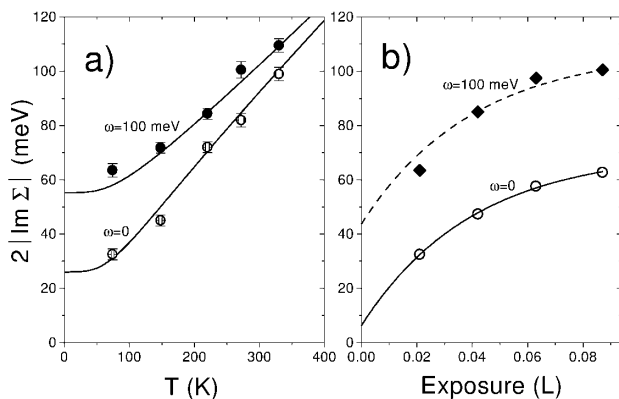


FIG. 4. The peak width as a function of (a) temperature and (b) exposure to background hydrogen, measured for two binding energies. For the exposure dependence the sample was held at 70 K. Lines in (a) are calculated electron-phonon contributions, shifted up by 26 meV to match the data. Lines in (b) represent fits (see text for details).

$T = 70$ K. However, we should also note that there is some uncertainty in the initial coverage due to the change in adsorption conditions between flashing the sample and the measurement.

In conclusion, we have analyzed the dispersion and the width of the Mo(110) surface state and isolated different mechanisms for scattering of the quasiparticle. For the first time it has been possible to isolate the electron-electron, electron-phonon, and electron-impurity scattering contributions to the quasiparticle lifetime. The electron-electron contribution is shown to be an order of magnitude higher than that for s - p -derived states. Our study shows that ARPES offers the possibility of momentum resolving the electron-phonon contribution to the real and imaginary parts of the self-energy.

This work is supported by the U.S. Department of Energy (DOE) under Contract No. DE-AC02-98CH10886.

-
- [1] D. Pines and P. Nozières, *The Theory of Quantum Liquids* (Benjamin, New York, 1969).
 - [2] G. Grimvall, *The Electron-Phonon Interaction in Metals* (North-Holland, New York, 1981).
 - [3] C. Bourbonnais *et al.*, J. Phys. Lett. **45**, L755 (1984); B. Dardel *et al.*, Europhys. Lett. **24**, 687 (1993).
 - [4] C. G. Olson *et al.*, Phys. Rev. B **42**, 381 (1990).
 - [5] M. Gurvitch and A. T. Fiory, Phys. Rev. Lett. **59**, 1337 (1987).
 - [6] G. A. Tomas *et al.*, Phys. Rev. Lett. **61**, 1313 (1988).
 - [7] J. Li *et al.*, Phys. Rev. Lett. **81**, 4464 (1998).
 - [8] W. Nessler *et al.*, Phys. Rev. Lett. **81**, 4480 (1998).
 - [9] In sudden approximation ARPES intensity is given by $I(\mathbf{k}, \omega) = |M(\mathbf{K}, \omega)|^2 A(\mathbf{k}, \omega) f(\omega)$, where $A(\mathbf{k}, \omega)$ is the spectral function, $f(\omega)$ is the Fermi function, and $M(\mathbf{k}, \omega)$ is a slowly varying term containing matrix elements for photoemission.
 - [10] B. A. McDougall, T. Balasubramanian, and E. Jensen, Phys. Rev. B **51**, 13891 (1995); T. Balasubramanian *et al.*, Phys. Rev. B **57**, R6866 (1998); P. Hofmann *et al.*, Phys. Rev. Lett. **81**, 1670 (1998).
 - [11] R. Claessen *et al.*, Phys. Rev. Lett. **69**, 808 (1992).
 - [12] C. Hodges, H. Smith, and J. W. Wilkins, Phys. Rev. B **4**, 302 (1971).
 - [13] K. Jeong, R. H. Gaylord, and S. D. Kevan, Phys. Rev. B **38**, 10302 (1988); **39**, 2973 (1989).
 - [14] J. B. Pendry, in *Photoemission and the Electronic Properties of Surfaces*, edited by B. Feuerbacher, B. Fitton, and R. F. Willis (Wiley, New York, 1978).
 - [15] S. Y. Savrasov and D. Y. Savrasov, Phys. Rev. B **54**, 16487 (1996).
 - [16] J. Kröger, S. Lehwald, and H. Ibach, Phys. Rev. B **55**, 10895 (1997).
 - [17] W. A. Harrison, *Electronic Structure and the Properties of Solids* (W. H. Freeman & Co., San Francisco, 1980).